Infrared Spectroscopy of the Pentacoordinated Carbonium Ion $C_2H_7^+$

L. I. Yeh, J. M. Price, and Y. T. Lee*

Contribution from the Department of Chemistry, University of California, Berkeley, California 94720, and Materials and Chemicals Sciences Division, Lawrence Berkeley Laboratory, 1 Cyclotron Road, Berkeley, California 94720.
Received February 21, 1989

Abstract: The infrared spectrum of $C_2H_7^+$ has been obtained from 2500 to 4200 cm^{-1}. The apparatus consists of a tandem mass spectrometer with a radio-frequency octopole ion trap. After initial mass selection of the $C_2H_7^+$ in a sector magnet, the $C_2H_7^+$ is spectroscopically probed by using a two-color laser scheme while being trapped under ultrahigh-vacuum conditions. The first laser is scanned from 2500 to 4200 cm^{-1} and excites a C–H stretching vibration. The second laser is a continuous-wave CO_2 laser and is used to dissociate the vibrationally excited parent ions through a multiphoton process. The fragment ion $C_2H_5^+$ is detected by using a quadrupole mass spectrometer. Two sets of spectral features were studied that showed different dependences on the backing pressure in the ion source, on the mixing ratio of hydrogen to ethane, and on the presence or absence of the second laser. Arguments are presented that the two groups of bands can be assigned to the classical and bridging structures of $C_2H_7^+$.

Gas-phase ion spectroscopy, though still a relatively young field, can now be used to probe molecular ions of increasing complexity by making use of improved technology and novel approaches. One of these new methods, recently developed in our laboratory,[1] uses a two-color laser scheme to probe the mass-selected ions trapped in a radio-frequency octopole field. The first laser is a tunable infrared laser that is used to excite the vibrations of the molecular ion of interest. The second laser is a CO_2 laser that is used to dissociate the vibrationally excited parent ion. It is possible to obtain the infrared spectrum by monitoring the formation of fragment ions as a function of the frequency of the tunable laser. This technique has not only allowed us to study the vibrational spectrum of hydrated hydronium ions but also allowed us to study the pentacoordinated carbonium ion $C_2H_7^+$.

A great deal of effort has been expended to study carbonium ions. In the early work, a need arose to explain rearrangement of carbonium ions, such as the norbornyl cation in solution. Hydrogen migration to form a σ-bonded intermediate was proposed. This intermediate, which contains a two-electron three-center bond, was given the name "nonclassical" ion. A pioneer in these studies was S. Winstein. In 1952, he reported an interesting solvolysis study of *endo*- and *exo*-norbornyl arylsulfonates.[2,3] Acetolysis yields the *exo*-norbornyl acetate, independent of whether the starting diastereomer was of the endo or exo configuration. In a complementary experiment, solvolysis of optically active *exo*-norbornyl *p*-bromobenzenesulfonate gave a product mixture that was shown to be racemic by the loss of optical activity.[3] A third observation was the enhanced rate of reaction of the exo isomer over the endo isomer.[3] All of these anomalies could be explained by a bridged structure for the norbornyl cation containing a pentavalent carbon. Bridged structures such as this, which have delocalized bonding σ-electrons, are now known as nonclassical ions.[4]

This concept of nonclassical ions was generally accepted when applied to the norbornyl and many other systems until 1962, when H. C. Brown strongly objected.[4,5] He claimed that scientific scrutiny had been bypassed in the general labeling of many ions as nonclassical. Other theories could also explain the anomalous behavior, so the nonclassical interpretation did not need to hold for every case.

Brown proposed alternative explanations for the controversial experimental observations.[5] One possibility was that two interchanging asymmetric classical structures go through a nonclassical structure momentarily. This indeed seemed to be possible for a number of systems where an asymmetric product is obtained from an isotopically tagged reactant with negligible scrambling of the tag.[6] This test is only suggestive, not conclusive, and will be informative only when the equilibration of the two distinctly tagged structures is not more rapid than the identification process chosen. Another possibility was that the bridged form was a transition state with a very low barrier, allowing facile rearrangement.[5] Brown also believed a clarification needed to be made between σ-bridging and hyperconjugation. G. Olah has also emphasized this point.[7] In both σ-bridging and hyperconjugation a σ-bond orbital and p-orbital overlap to allow electron delocalization involving that σ-bond. When there is little or no rearrangement of the nuclei, this is called hyperconjugation. When there is extensive nuclear reorganization, this is called bridging.[7] In 1975, G. Olah[7] proclaimed that he had proven the existence of the nonclassical norbornyl cation using NMR techniques and settled that question.

Subsequently, the problem to be addressed then becomes which carbonium ions have this nonclassical structure? Candidates include the pentacoordinated protonated ethane and nonsaturated alkanes such as protonated acetylene and protonated ethylene. Classical and bridged structures for these three carbonium ions are shown schematically in Figure 1.

$C_2H_7^+$ was seen in the 1960s with a discharge of methane and/or ethane in mass spectrometric studies.[8–11] It was clear that $C_2H_7^+$ easily dissociated to give $C_2H_5^+ + H_2$ products. Olah et al.[12] observed pentacoordinated carbon cations in acid solution using NMR. This pointed out the importance of carbonium ions in solution chemistry. Blair et al.[13] observed $C_2H_7^+$ in an ion trap using a continuous electron beam to trap the ions through negative space charge. The quantity of $C_2H_7^+$ increased with trapping time.

* To whom correspondence should be addressed at the Department of Chemistry, University of California.

(1) Yeh, L. I.; Okumura, M.; Myers, J. D.; Lee, Y. T. NAS Workshop on Molecular and Cluster Beam Science; National Academy Press: Washington, D.C., 1988; p 57. Yeh, L. I.; Okumura, M.; Myers, J. D. Price, J. M.; Lee, Y. T., submitted.
(2) Winstein, S.; Trifan, D. *J. Am. Chem. Soc.* **1952**, *74*, 1147.
(3) Winstein, S.; Trifan, D. *J. Am. Chem. Soc.* **1952**, *74*, 1154.
(4) Morrison, R. T.; Boyd, R. N. *Organic Chemistry*; Allyn and Bacon: Boston, 1973; pp 917–918.
(5) Brown, H. C. *Tetrahedron* **1976**, *32*, 179.
(6) Roberts, J. D.; Yancey, J. A. *J. Am. Chem. Soc.* **1952**, *74*, 5943.
(7) Olah, G. A. *Acc. Chem. Res.* **1976**, *9*, 41.
(8) Wexler, S.; Jesse, N. *J. Am. Chem. Soc.* **1962**, *84*, 3425.
(9) Field, F. H.; Franklin, J. L.; Munson, M. S. B. *J. Am. Chem. Soc.* **1963**, *85*, 3575.
(10) Munson, M. S. B.; Franklin, J. L.; Field, F. H. *J. Phys. Chem.* **1964**, *68*, 3098.
(11) Munson, M. S. B.; Field, F. H. *J. Am. Chem. Soc.* **1965**, *87*, 3294.
(12) Olah, G. A.; Klopman, G.; Schlosberg, R. H. *J. Am. Chem. Soc.* **1969**, *91*, 3261.
(13) Blair, A. S.; Heslin, E. J.; Harrison, A. G. *J. Am. Chem. Soc.* **1972**, *94*, 2935.

0002-7863/89/1511-5597$01.50/0

Table I. Relative Energies of the Classical (cl) and Bridged (br) Structures of $C_2H_3^+$, $C_2H_5^+$, and $C_2H_7^+$, Heats of Formation for $C_2H_7^+$, and Proton Affinities for C_2H_6 (Units Are kcal/mol)

ref	$C_2H_3^+$ (cl–br)	$C_2H_5^+$ (cl–br)	$C_2H_7^+$ (cl–br)	$H_f(C_2H_7^+)$	$PA(C_2H_6)$
Lathan et al.[a]		−7	9.8		140.1
Hariharan et al.[b]	−5.7	1			
Chong and Franklin[c]				218.8 ± 1	127.0 ± 1
Bohme et al.[d]					136 < PA < 159
Zurawski et al.[e]	7	9			
Bischof and Dewar[f]			−15	199.8 (cl), 215 (br)	
Kohler and Lischka[g]			−11 (MINDO), 8.5 (SCF), 6.3 (CEPA)		138.3 (cl), 143.4 (br)
French and Kebarle[h]				208.5 ± 2 (br)	137.4 ± 2 (br)
Hiraoka and Kebarle[i]			7.8	215 (cl), 207.2 (br)	131.8 (cl), 139.6 (br)
Houle and Beauchamp[j]		~3			
Mackay et al.[k]				204.8 ± 1	142.1 ± 1
Weber and McLean[l]	1–2				
Lischka and Kohler[m]	5.3 (MINDO), 4.0 (CEPA)	8.0			
		7.3			
Kohler and Lischka[n]	3.5–4.0				
Raghavachari et al.[o]	3.0	6.5	6.8		
Hirao and Yamabe[p]	1.30	4.11	4.03		135.6 (cl), 139.7 (br)

[a] Reference 14. [b] Reference 15. [c] Reference 16. [d] Reference 17. [e] Reference 18. [f] Reference 20. [g] Reference 21. [h] Reference 22. [i] Reference 25. [j] Reference 26. [k] Reference 29. [l] References 30 and 31. [m] Reference 36. [n] Reference 32. [o] Reference 33. [p] Reference 34. [q] Reference 35.

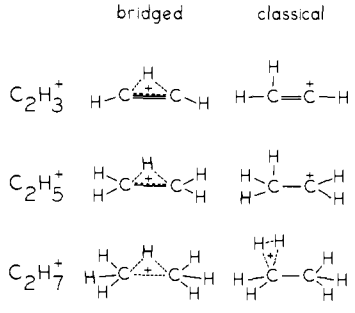

Figure 1. Schematic of bridged and classical structures for protonated acetylene, ethylene, and ethane.

In the early 1970s, Lathan, Hehre, and Pople[14] calculated the relative energies of bridged and classical forms of $C_2H_3^+$, $C_2H_5^+$, and $C_2H_7^+$. They used molecular orbital self-consistent field (MO-SCF) theory with small (STO-3G, 4-31G) basis sets and concluded that the classical structure of $C_2H_3^+$ was more stable by far compared to the bridged conformer. The classical form of $C_2H_5^+$ was also more stable than the bridged form (by 7 kcal/mol). However, calculations on $C_2H_7^+$ showed the bridged structure to be more stable by almost 10 kcal/mol. Hariharan, Lathan, and Pople[15] later found a preferential stabilizing effect of polarization functions on the bridged form over the classical. For $C_2H_3^+$, the classical structure was still found to be more stable, but by only 5.7 kcal/mol. In the case of $C_2H_5^+$, however, the bridged structure became the more stable conformer by ~1 kcal/mol when d-functions were included on C and p-functions on H.

Meanwhile, Chong and Franklin[16] made the controversial claim that $C_2H_7^+$ was less stable than $C_2H_5^+ + H_2$ and invoked an activation barrier to explain observation of $C_2H_7^+$. This led to a paper by Bohme et al.[17] in disagreement, contending that $C_2H_7^+$ was more stable than $C_2H_5^+ + H_2$. They used CO and C_2H_4 to bracket the proton affinity of ethane between 136 and 159 kcal/mol.

Zurawski, Alrichs, and Kutzelnigg[18] produced a landmark paper in 1973 when the effects of electron correlation were studied using the independent-electron-pair approximation based on the direct calculations of pair-natural orbitals (IEPA PNO). Polarization functions were again found to be very important to stabilize the bridged structure, and electron correlation further preferentially stabilized the nonclassical form by an equally substantial amount. They found the bridged structure to be more stable than the classical for both $C_2H_3^+$ and $C_2H_5^+$ (by 7 and 9 kcal/mol, respectively). The IEPA method was also used to calculate the relative energies of the C_s and C_{2v} geometries in CH_5^+ by Dyczmons and Kutzelnigg.[19] Whereas at the SCF level the C_s structure was more stable, including electron correlation energy led to equal stabilities of the two. Semiempirical methods were used in 1975 by Bischof and Dewar[20] to calculate the relative stabilities of $C_2H_7^+$. They found the classical form more stable by 15 kcal/mol. This is clearly at odds with ab initio calculations. Nevertheless, Bischof and Dewar came out in strong defense of the MINDO/3 method. This led to work by Kohler and Lischka[21] comparing SCF, coupled electron pair approximation (CEPA) PNO, and MINDO/3 calculations on the $C_2H_7^+$ ion. At the SCF and CEPA PNO levels, the bridged structures were more stable by 8.5 and 6.3 kcal/mol, respectively. However, at the MINDO/3 level, the classical $C_2H_7^+$ structure was more stable than the bridged form by 11 kcal/mol. This shows the inadequacy of the MINDO/3 method in calculating relative energies for protonated ethane.

Very influential experiments from Kebarle's lab came out in 1975–1976.[22-25] French and Kebarle[22] studied the pyrolysis of $C_2H_7^+$ and found an activation energy of 10.5 kcal/mol for dissociation into $C_2H_5^+ + H_2$. They concluded that $PA(C_2H_6)$ was greater than $PA(CH_4)$ by more than 10 kcal/mol. Assuming the activation energy for the reaction equals the enthalpy change, they found $\Delta H_f(C_2H_7^+) = 208.5 \pm 2$ kcal/mol and $PA(C_2H_6) = 137.4 \pm 2$ kcal/mol. This was confirmed by experiments done by Hiraoka and Kebarle[25] in which they claimed to observe both the classical and nonclassical forms as a function of temperature. At the lowest temperature range they found the reaction of $C_2H_5^+ + H_2 \rightarrow C_2H_7^+$ had an inverse temperature relationship, implying it was exothermic. At higher temperatures, the temperature dependence became positive, suggesting an endothermic relationship. Analyzing these temperature dependences led to the conclusions shown in Figure 2. The bridged structure is more stable than the classical by 7.8 kcal/mol. This leads to ΔH_f(bridged $C_2H_7^+$) = 207.2 kcal/mol, ΔH_f(classical $C_2H_7^+$) = 215.0

(14) Lathan, W. A.; Hehre, W. J.; Pople, J. A. *J. Am. Chem. Soc.* **1971**, *93*, 808.
(15) Hariharan, P. C.; Lathan, W. A.; Pople, J. A. *Chem. Phys. Lett.* **1972**, *14*, 385.
(16) Chong, S. L.; Franklin, J. L. *J. Am. Chem. Soc.* **1972**, *94*, 6347.
(17) Bohme, D. K.; Fennelly, P.; Hemsworth, R. S.; Schiff, H. I. *J. Am. Chem. Soc.* **1973**, *95*, 7512.
(18) Zurawski, B.; Ahlrichs, R.; Kutzelnigg, W. *Chem. Phys. Lett.* **1973**, *21*, 309.
(19) Dyczmons, V.; Kutzelnigg, W. *Theor. Chim. Acta* **1974**, *33*, 239.
(20) Bischof, P. K.; Dewar, M. J. S. *J. Am. Chem. Soc.* **1975**, *97*, 2278.
(21) Kohler, H.-J.; Lischka, H. *Chem. Phys. Lett.* **1978**, *58*, 175.
(22) French, M.; Kebarle, P. *Can. J. Chem.* **1975**, *53*, 2268.
(23) Hiraoka, K.; Kebarle, P. *J. Chem. Phys.* **1975**, *63*, 394.
(24) Hiraoka, K.; Kebarle, P. *Can. J. Chem.* **1975**, *53*, 970.
(25) Hiraoka, K.; Kebarle, P. *J. Am. Chem. Soc.* **1976**, *98*, 6119.

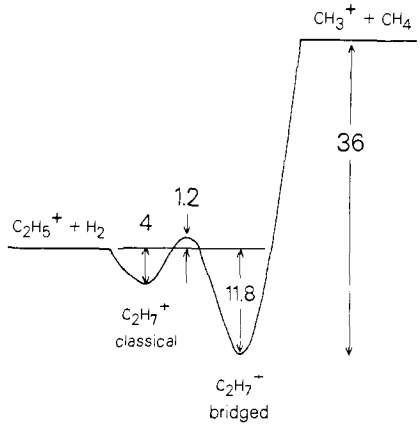

Figure 2. Energy diagram based on the thermochemical studies of ref 25 for the bridged and classical forms of $C_2H_7^+$.

kcal/mol, and PA(C_2H_6 → bridged $C_2H_7^+$) = 139.6 kcal/mol, PA(C_2H_6 → classical $C_2H_7^+$) = 131.8 kcal/mol. These values are summarized in Table I.

An experimental study by Houle and Beauchamp[26] of the difference between the adiabatic and vertical ionization potentials of ethyl radical led to an estimated 3 kcal/mol difference between the bridged and classical structures of $C_2H_5^+$, with the bridged being lower. Their assumption was that a vertical ionization of ethyl radical would lead to the classical structure of ethyl cation, whereas the adiabatic ionization would end with the lower energy bridged structure which necessitates a large geometry change. Houle and Beauchamp obtained a heat of formation for $C_2H_5^+$ of 219.2 ± 1.1 kcal/mol. This is in some disagreement with the value of 215.3 ± 1.0 kcal/mol found by Baer,[27] who did a photoionization and photoion–photoelectron coincidence (PIPECO) study of $C_2H_5^+$ formation. It is conceivable that the very large geometry change between the ethyl radical and the bridged ethyl cation makes it impossible to obtain a true adiabatic ionization potential experimentally. Gellene, Kleinrock, and Porter[28] took the reverse approach in that they started with the ethyl cation and neutralized it using various metals. They claimed that 87–90% of their $C_2H_5^+$ beam was the bridged structure. From this they put a lower bound on the difference in energy between the bridged and classical structures as 0.8 kcal/mol. Mackay, Schiff, and Bohme[29] studied the energetics and kinetics of the protonation of ethane. They obtained $\Delta H_f(C_2H_7^+)$ = 204.8 ± 1.3 kcal/mol and PA(C_2H_6) = 142.1 ± 1.2 kcal/mol, which presumably corresponds to the bridged form.

More recent theoretical calculations have generally concluded that the bridged structure is more stable than the classical for all three of the carbonium ions: $C_2H_3^+$, $C_2H_5^+$, and $C_2H_7^+$. The energies for the two structures are closest for $C_2H_3^+$. Weber and McLean,[30,31] using configuration interaction (SDCI) and a double-ζ plus polarization (DZ + P) basis set, found bridged and classical $C_2H_3^+$ structures to have energies within 1–2 kcal/mol, with the bridged form probably lower. Kohler and Lischka[32] included electron correlation using CEPA and found the bridged structure of protonated acetylene lower by 3.5–4.0 kcal/mol. Raghavachari, Whiteside, Pople, and Schleyer[33] found the bridged form lower by ~3.0 kcal/mol, and more recent calculations by Hirao and Yamabe[34] found the bridged structure of $C_2H_3^+$ to be lower by 1.30 kcal/mol using the symmetry-adapted cluster method with zero-point energy correction (SAC + ZPE). These values are in close agreement with the more recent calculations by Lee and Schaefer,[35] who found an energy difference of 0.97 kcal/mol using CISDT (DZ + P). Calculations on $C_2H_5^+$ found larger energy differences. Lischka and Kohler[36] found the bridged structure lower by 7.3 kcal/mol using the ab initio CEPA method and 8.0 kcal/mol using semiempirical MINDO/3. Raghavachari et al.[33] found the classical structure was not a minimum on the potential surface at the best level of theory considered (MP4(SDQ) with a reoptimization of the geometries at the MP2 level). With the geometries optimized at the HF level and MP4(SDQ), the bridged structure was lower than the classical by 5.2 kcal/mol. Hirao and Yamabe[34] found an energy difference of 4.11 kcal/mol. Following this trend, the bridged structure of $C_2H_7^+$ was also found to be significantly more stable than the classical structure. Raghavachari et al.[33] found an energy difference of 6.8 kcal/mol, while Hirao and Yamabe[34] found the bridged form lower by 4.0 kcal/mol. These results are also summarized in Table I.

Table II. Bond Lengths and Bond Angles of the Bridged and Classical Forms of Protonated Ethane as Given by Hirao and Yamabe[34] and Dupuis[41] (Bond Lengths Are Given in Angstroms, and Bond Angles Are in Degrees)[a]

bridged	Hirao and Yamabe	Dupuis
C–C	2.209	2.099
C–H_p	1.239	1.234
C–H_a, C–H_b	1.073–1.079	1.073–1.080
H_p to center of C–C	0.561	0.649
C–H_p–C	126.2	116.5
classical	**Hirao and Yamabe**	**Dupuis**
C–C	1.525	1.544
C–H_a	1.081	1.080
C–$H_{a'}$	1.082	1.082
C–H_b	1.086	1.078
C–H_1, C–H_2	1.267	1.295, 1.315
H_1–H_2	0.833	0.824
H_1–C–H_2	38.4	36.8

[a] H_a and H_b are on opposite carbons and H_p is the bridging proton in the nonclassical structure. In the classical structure, the two hydrogens in the H_2 moiety are labeled 1 and 2. The other two hydrogens on the same carbon are labeled H_b. Two of the hydrogens on the opposite carbon are labeled H_a, and the third is labeled $H_{a'}$.

In the past few years, calculations of vibrational frequencies have been done. Raine and Schaefer[37] calculated vibrational frequencies, intensities, and geometries using SCF with a DZ + P basis set of both the classical and nonclassical forms of $C_2H_3^+$. This was followed by a calculation by Lee and Schaefer[35] at a higher level of theory that gave similar results on vibrational frequencies. The motivation for repeating this calculation was to aid in the assignment of the spectrum experimentally observed by Crofton and Oka.[38] This infrared spectrum is now assigned as essentially that of the bridged structure, possibly with some complications associated with tunneling between the nonclassical and classical forms. DeFrees and McLean[39] also completed vibrational frequency calculations of protonated acetylene. In addition, they calculated frequencies for nonclassical $C_2H_5^+$ and CH_5^+. In 1987, Komornicki and Dixon[40] calculated frequencies, intensities, and structures for CH_5^+. M. Dupius[41] has probably done the highest level calculation on CH_5^+ to date. At our request, Dupius[41] has also calculated frequencies and intensities for classical and bridged protonated ethane. The frequencies, intensities, and assignments will be discussed later.

The intriguing work of Kanter, Vager, Both, and Zajfman[42] should also be mentioned. They succeeded in experimentally

(26) Houle, F. A.; Beauchamp, J. L. *J. Am. Chem. Soc.* **1979**, *101*, 4067.
(27) Baer, T. *J. Am. Chem. Soc.* **1980**, *102*, 2482.
(28) Gellene, G. I.; Kleinrock, N. S.; Porter, R. F. *J. Chem. Phys.* **1983**, *78*, 1795.
(29) Mackay, G. I.; Schiff, H. I.; Bohme, D. K. *Can. J. Chem.* **1981**, *59*, 1771.
(30) Weber, J.; McLean, A. D. *J. Am. Chem. Soc.* **1976**, *98*, 875.
(31) Weber, J.; Yoshimine, M.; McLean, A. D. *J. Chem. Phys.* **1976**, *64*, 4159.
(32) Kohler, H.-J.; Lischka, H. *Theor. Chim. Acta* **1979**, *54*, 23.
(33) Raghavachari, K.; Whiteside, R. A.; Pople, J. A.; Schleyer, P. v. R. *J. Am. Chem. Soc.* **1981**, *103*, 5649.
(34) Hirao, K.; Yamabe, S. *Chem. Phys.* **1984**, *89*, 237.
(35) Lee, T. J.; Schaefer, III, H. F. *J. Chem. Phys.* **1986**, *85*, 3437.
(36) Lischka, H.; Kohler, H.-J. *J. Am. Chem. Soc.* **1978**, *100*, 5297.
(37) Raine, G. P.; Schaefer III, H. F. *J. Chem. Phys.* **1984**, *81*, 4034.
(38) Crofton, M.; Oka, T., private communication.
(39) DeFrees, D. J.; McLean, A. D. *J. Chem. Phys.* **1985**, *82*, 333.
(40) Komornicki, A.; Dixonn, D. A. *J. Chem. Phys.* **1987**, *86*, 5625.
(41) Dupuis, M., private communication.
(42) Kanter, E. P.; Vager, Z.; Both, G.; Zajfman, D. *J. Chem. Phys.* **1986**, *85*, 7487.

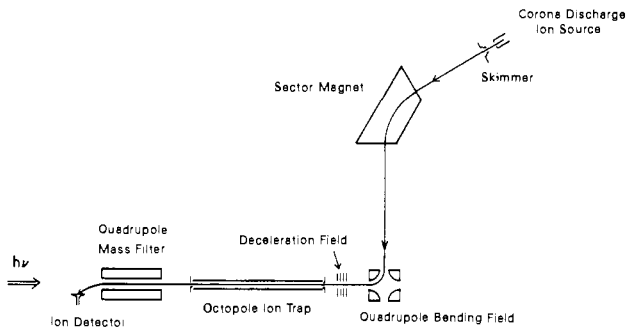

Figure 3. Schematic of the experimental apparatus.

determining the structure of $C_2H_3^+$ through a Coulomb explosion of the $C_2H_3^+$ ion caused by the sudden loss of several electrons. The arrival times of the three protons and two carbon ions are detected with both X–Y spatial resolution and temporal resolution and analyzed to give average geometries. They find the nonclassical structure dominates their sample of $C_2H_3^+$.

Thus, it seems certain that the lower energy structure after protonating acetylene, ethylene, and ethane is the nonclassical bridged form. Our work concentrated on the spectroscopy of protonated ethane. After a description of the experimental setup and spectra obtained, convincing arguments will be presented to show that spectra have been obtained for both the bridged and classical structures. Table II lists bond lengths and angles for both forms of $C_2H_7^+$ as calculated by Hirao and Yamabe[34] and by Dupius.[41]

Experimental Details

The apparatus used has been described previously.[43] A schematic of the machine is given in Figure 3. Briefly, the ions are formed in a corona discharge and then mass-selected in a sector magnet. The ion under study is then trapped in an octopole radio-frequency (rf) ion trap for 1 ms, during which time they are interrogated by a tunable IR laser. Since the density of $C_2H_7^+$ in the trap is not high enough to allow the direct measurement of photon absorption, the vibrational excitation of $C_2H_7^+$ was detected by using a continuous-wave (cw) CO_2 laser to dissociate vibrationally excited $C_2H_7^+$ into $C_2H_5^+ + H_2$. The $C_2H_5^+$ ions are then selected by a quadrupole mass filter and counted by a Daly scintillation ion counter.[44]

In this experiment, it was seen that the spectrum was strongly dependent on the mixing ratio and backing pressure behind the nozzle. Hydrogen:ethane ratios were systematically varied from 55 000:1 to 8700:1. Backing pressures used were 60, 90, and 150 Torr. The gases used were Matheson ultrahigh-purity hydrogen (99.999%) and pure ethane from Spectra Gases (99.99%). In spite of this high purity, we found it helpful to remove residual water by flowing the gas through a molecular sieve trap (Linde 13× molecular sieve, 10-Å pore diameter) cooled in a dry ice/acetone bath before allowing the gas to enter the source.

A schematic of the corona discharge ion source is shown in Figure 4. The discharge is struck between the nickel-plated iron needle and the copper walls of the source. The distance between the needle and the source body was 0.069 ± 0.003 in. The source body was composed primarily of copper for more efficient cooling from a refrigerant that was introduced from outside the machine and used to cool a copper block that was clamped around the base of the source. For this experiment, Freon-22 was used to cool the source to −28 °C. This was necessary to freeze out impurity water contained in the gas inlet line. At the highest pressure, contamination was more of a problem, and the source had to be warmed up after running for only a few hours to allow the condensed water to be pumped off from the surfaces.

After the discharge and before the nozzle is a small high-pressure drift region that allows the ions to cool vibrationally through multiple collisions. A supersonic expansion through a 75-μm nozzle cools the rotational temperature to ≤40 K. About 7.5-mm downstream from the nozzle is a skimmer that separates the first and second regions of differential pumping. Typical pressures before and after the skimmer are

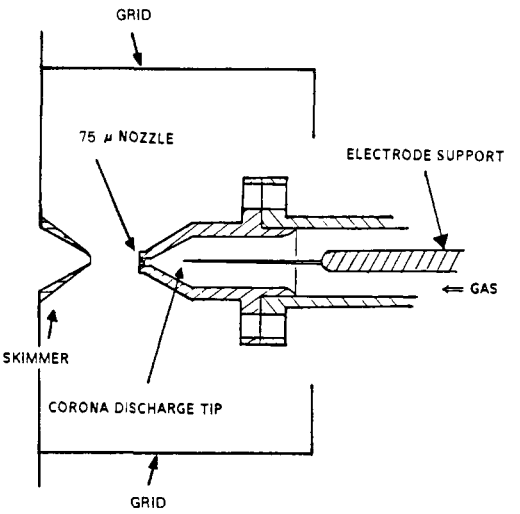

Figure 4. Ions created in a corona discharge ion source. Typical conditions are described in the text.

1.1×10^{-4} and 8.4×10^{-6} Torr when run with a backing pressure of 90 Torr. The voltage bias of the nozzle and skimmer was kept within 1.0 V of each other to minimize collisional heating by accelerating ions in this higher pressure region.

In the lower pressure region after the skimmer, the ions are gradually accelerated to a kinetic energy of 350 eV, which they maintain (through the sector magnet) until directly before the ion trap. To keep the machine at ground potential, the ion source and associated optics and the ion trap are floated at +350 V. A stack of 12 evenly spaced plate lenses decelerate the ions before entering the octopole trap.[45] In the trap, their kinetic energy is less than 0.5 eV. The octopole trap consists of eight molybdenum rods 50 cm long, 0.32 cm in diameter, evenly spaced on a 1.25-cm-diameter circle. Alternate rods have, at any moment, opposite phases of rf applied with typically 300-V peak-to-peak and a frequency of 7.4 MHz.

The tunable infrared laser is a Quanta-Ray infrared wavelength extender system (IR-WEX) which is scanned from 2490 to 4150 cm^{-1}. The infrared wavelength is generated in a lithium niobate crystal that takes the difference of a Quanta-Ray pulsed dye laser (PDL) output and a Nd:YAG fundamental. Scanning is achieved by a computer-controlled motor system that steps the drive for the dye laser grating. In the high-resolution scans, an etalon was placed in the Nd:YAG cavity which reduced the IR line width from 1.2 to 0.3 cm^{-1}. Pulse duration was 10 ns with typically 0.5 mJ/pulse at 2800 cm^{-1} and 1 mJ/pulse at 3940 cm^{-1}.

The WEX output was combined with a cs MPB Technologies Inc. CO_2 laser using a custom-designed beam combiner on a ZnSe substrate (CVI Laser Corp.). The CO_2 laser was run on the R(10) line of the 00^01–10^00 band with 6–8 W at the output of the laser and with 3–4 W passing completely through the machine. This was used to selectively dissociate those ions vibrationally excited by the WEX. The method of selective dissociation of vibrationally excited $C_2H_7^+$ is mainly based on the difference in the density of states near $v = 0$ and $v = 1$, which causes enhanced multiphoton dissociation (MPD) of $v = 1$ as compared to $v = 0$. Because spectroscopy is done in this apparatus through detection of fragment ions, it is important to have a strong correlation between vibrational excitation of parent ions and formation of fragment ions. This has been achieved in this experiment by monitoring the fragment ion $C_2H_5^+$.

Results

All of the $C_2H_7^+$ spectroscopy was done by monitoring formation of $C_2H_5^+$ as a function of the WEX frequency. The spectra obtained from 2500 to 3400 cm^{-1} at 60, 90, and 150 Torr and a mixing ratio of 45 00:1 hydrogen to ethane are shown in Figure 5. The five features at lower frequencies (2521, 2601, 2683, 2762, and 2825 cm^{-1}) disappear with increasing source backing pressure, while the higher frequency features (2945, 3082, and 3128 cm^{-1}) remain unaffected. The intensities of the peaks to the red of 2900 cm^{-1} also drop dramatically when the amount of ethane compared to hydrogen is increased by a factor of 5 (H_2:C_2H_6 of 8700:1). Yet a third way to distinguish the two sets of features is to block

(43) See also: Bustamente, S. W. Ph.D. Thesis, University of California, Berkeley, California, 1983. Okumura, M. Ph.D. Thesis, University of California, Berkeley, California, 1986.

(44) Daly, N. R. *Rev. Sci. Instrum.* **1960**, *31*, 264. See also: Lee, Y. T.; McDonald, J. D.; LeBreton, P. R.; Herschbach, D. R. *Ibid.* **1969**, *40*, 1402.

(45) Teloy, E.; Gerlich, D. *Chem. Phys.* **1974**, *4*, 417.

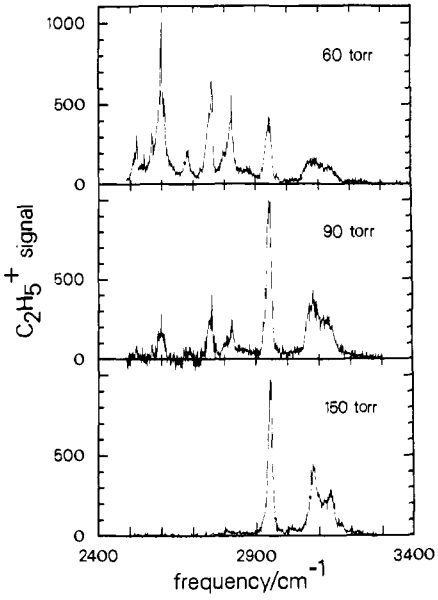

Figure 5. Spectrum of $C_2H_7^+$ from 2500–3300 cm^{-1} taken by using a hydrogen to ethane ratio of 45 000:1 at the backing pressures indicated. The features that disappear with increasing pressure are due to the classical structure of $C_2H_7^+$. The bands that are independent of pressure are from the more stable bridging structure of $C_2H_7^+$.

Table III. Experimentally Observed Vibrational Frequencies (cm^{-1}) of $C_2H_7^+$

freq	shows pressure dependence	remains when CO_2 is blocked	freq	shows pressure dependence	remains when CO_2 is blocked
3964.0	yes	yes	3082	no	no
3917	no	yes	2945.4	no	no
3845	no	yes	2825	yes	yes
3762	no	yes	2762.2	yes	yes
3726	no	yes	2683	yes	yes
3667	no	yes	2601	yes	yes
3128	no	no	2521	yes	yes

the CO_2 laser and have only the WEX passing through the machine. This causes the higher frequency peaks to disappear but leaves the peaks below 2900 cm^{-1} apparently unaffected. This implies that some of the parent ions that are associated with the five features below 2900 cm^{-1} are able to predissociate after the absorption of a single tunable IR photon. These results are summarized in Table III.

The scanning range was extended later to cover the frequencies from 3400 to 4200 cm^{-1} as shown in Figure 6. An additional band at 3964 cm^{-1} was also found to be dependent on the source conditions used. Also, several more features were seen that were not dependent on the backing pressure. A broad intense band centered around 3845 cm^{-1} dominates this region. Two sharp features at 3667 and 3917 cm^{-1} are also quite prominent. The features at 3726 and 3762 cm^{-1} are much less intense. All five of these features appear pressure independent as seen in Figure 6. In contrast to earlier results, however, these features are independent of whether the CO_2 laser is on or off. Frequencies of all of the experimentally observed peaks are given in Table III. Both the backing and pressure dependence and CO_2 laser dependence are also included.

Attempts at higher resolution spectra were made by inserting the etalon in the YAG, yielding approximately a factor of 4 reduction in line width. The bands centered at 2945.4 and 2762.2 cm^{-1} showed no resolvable structure within the signal-to-noise level, although their band envelopes are distinctly different. However, the band at 3964.0 cm^{-1} is clearly separated into a P, Q, R subband structure as shown in Figure 7.

Discussion

The obvious question from the observed spectra is why there seems to be two sets of peaks based on pressure dependence. They

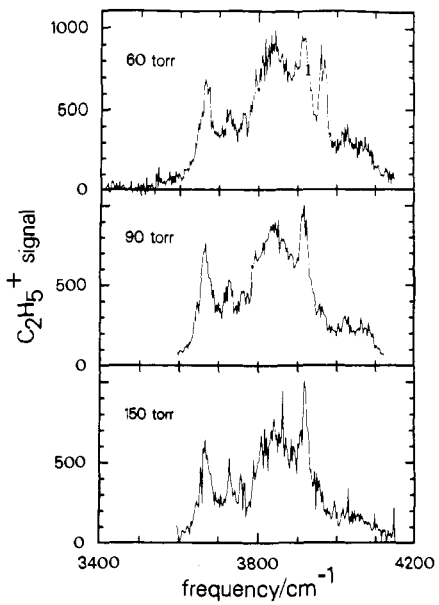

Figure 6. Spectrum of $C_2H_7^+$ from 3400 to 4100 cm^{-1} taken by using a hydrogen to ethane ratio of 45 000:1 at the backing pressures indicated. The feature at 3964.0 cm^{-1} disappears with increasing pressure and is assigned to the H–H stretch of the classical structure of $C_2H_7^+$.

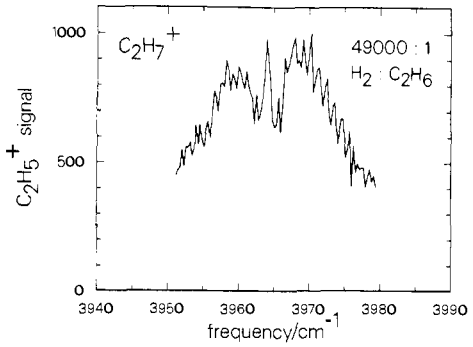

Figure 7. Higher resolution scan of the band centered at 3964.0 cm^{-1}. P, Q, R branches are emerging with some partial rotational resolution. The vibration excited is the H–H stretch in the classical structure of $C_2H_7^+$.

can come either from hot bands or from the presence of two $C_2H_7^+$ structures. The features below 3400 cm^{-1} will be considered separately from those above.

A. 2400–3400 cm^{-1}. From energetic considerations, hot bands would be expected to need less energy to dissociate, in agreement with the above described observations for these features below 2900 cm^{-1}. Note that three of the bands below 2900 cm^{-1} are more intense than the strongest C–H stretch. We expect that the observed spectral intensities reflect the true intensities fairly well. This assumption depends on the following two facets to be true. First, no frequency dependence is introduced in the multiphoton excitation process by the CO_2 laser. This is most probably the case since no change in the spectrum is observed when the CO_2 laser is blocked. Second, the dissociation rate is fast enough that the variation upon excitation of different modes will not affect the observed spectrum. This is also a valid assumption since the RRKM lifetime is many orders of magnitude shorter than the 1-ms trapping time. This makes the hot band hypothesis seem unlikely. To have a hot band intensity be stronger than the fundamental, the excitation of the "hot" bend or stretch would have to significantly increase the transition moment of the C–H stretching vibration, since a population inversion is probably impossible.

The most likely reason is the presence of both the bridged and classical structures. The classical structure is higher in energy than the bridged by 4–8 kcal/mol.[25,33,34] This lends credence to the idea that the bridged structure will not dissociate after being

Table IV. Vibrational Frequencies and Intensities of the $C_2H_7^+$ Bridged Structure (Frequencies Are in cm^{-1}, Intensities Are in $D^2/(Å^2 \cdot amu)$)[a]

ν	species	calcd freq	int	obsd freq	assgnt
1	B	3466 (3119)	0.32		CH_a, CH_b asym stretch, out of phase
2	A	3466 (3119)	0.57	3128	CH_a, CH_b asym stretch, in phase
3	A	3422 (3080)	0.35		CH_a, CH_b asym stretch, in phase
4	B	3420 (3078)	0.65	3082	CH_a, CH_b asym stretch, out of phase
5	A	3275 (2947)	0.08		CH_a, CH_b sym stretch, in phase
6	B	3272 (2944)	0.37	2945.4	CH_a, CH_b sym stretch, out of phase
7	B	2305 (2074)	20.12		bridging proton, side to side
8	A	1984 (1786)	0.29		bridging proton, away from C–C bond
14	B	1345 (1210)	2.13		CH_a, CH_b deformation
17	B	1003 (900)	10.23		CH_a, CH_b rock

[a] Theoretical frequencies are from M. Dupuis.[41] Scaled frequencies are in parentheses. Predicted symmetry is C_2.

excited by the WEX unless the CO_2 laser is on, whereas the classical structure can dissociate. Thus, the five features below 2900 cm^{-1} seem to arise from the classical structure, and the features between 2900 and 3300 cm^{-1} from the bridged structure.

The five features at 2521, 2601, 2683, 2762, and 2825 cm^{-1} can be made to disappear both by raising the backing pressure and by increasing the relative amount of C_2H_6 to H_2. At the higher pressures, more collisions will occur behind the nozzle, which logically leads to more efficient internal cooling of the nascent ions. This leads to strongly enhanced formation of the lower energy bridged structure over the classical form. An analogous argument can be made for the case with a higher C_2H_6:H_2 ratio but the same backing pressure. Even though the number of collisions will be approximately the same, internally excited $C_2H_7^+$ is much more efficiently cooled through collisions with an ethane molecule than with a hydrogen molecule. Several mechanisms can contribute to this increased efficiency.[46,47] Due to the closer vibrational frequency match between C_2H_6 and $C_2H_7^+$ than between H_2 and $C_2H_7^+$, V → V transfer from the hot $C_2H_7^+$ will occur much more readily to ethane. Another factor is that ethane has a larger polarizability than hydrogen. This leads to an increased collision cross section through long-range ion-induced dipole forces. But, the most important quenching mechanism of the classical structure is likely to be proton transfer from a classical $C_2H_7^+$ to a C_2H_6 to form the more stable bridged $C_2H_7^+$. If this exothermic mechanism is not very efficient during the cooling process, some of the classical $C_2H_7^+$ will be trapped in the classical form and will not have enough energy to overcome the 5 kcal/mol barrier to isomerize into the bridged form.

M. Dupuis has calculated vibrational frequencies for both the bridged and classical forms of $C_2H_7^+$.[41] Comparison of his theoretically calculated vibrational frequencies with the experimental spectrum further supports the bridged/classical theory. Referring to Table IV, one sees that the SCF calculation for the bridged structure predicts six features above 2500 cm^{-1} with frequencies

Table V. Vibrational Frequencies and Intensities of the $C_2H_7^+$ Classical Structure (Frequencies Are in cm^{-1}, Intensities Are in $D^2/(Å^2 \cdot amu)$)[a]

ν	species	calcd freq	int	obsd freq	assgnt
1	A′	3516 (3164)	0.94	3964.0	H_1–H_2 stretch
2	A″	3434 (3091)	0.31	2825	CH_b–CH_b asym stretch
3	A″	3379 (3041)	0.04	2762.2	CH_a–CH_a asym stretch
4	A′	3363 (3027)	0.06	2683	$CH_{a'}$ stretch
5	A′	3328 (2995)	0.14	2601	CH_b–CH_b sym stretch
6	A′	3261 (2935)	0.04	2521	CH_a–CH_a sym stretch

[a] Theoretical frequencies are from M. Dupuis.[41] Scaled frequencies are in parentheses. Predicted symmetry is C_s.

3272, 3275, 3420, 3422, 3466, and 3466 cm^{-1}. These frequencies are expected to be 10% too high. Scaling them down yields the frequencies 2944, 2947, 3078, 3080, 3119, and 3119 cm^{-1}. Comparison with the experimental frequencies and intensities leads to the assignment of the 2945-cm^{-1} feature as mostly ν_6, the 3082-cm^{-1} feature to ν_3 and ν_4, and the 3128-cm^{-1} feature to ν_1 and ν_2. The agreement between the theoretical and experimental frequencies is excellent.

A comparison with the theoretical vibrational frequencies for the classical structure is also encouraging. The calculated frequencies and intensities are listed in Table V. The C–H bonds were treated at the SCF level, but the CH_1H_2 group was treated at the correlated level. Because of the difficulty of this calculation caused by the weakly bound H_2 group, absolute values for the frequencies may not be reliable. However, the separation between the asymmetric CH_a and CH_b peaks and the symmetric CH_a and CH_b peaks may prove more informative. This appears to be the case. The five experimental frequencies 2521, 2601, 2683, 2762, and 2825 cm^{-1} can be tentatively assigned to the five scaled frequencies 2935, 2995, 3027, 3041, and 3091 cm^{-1}. The experimental separation between the asymmetric CH_a and CH_b is 63 cm^{-1} as compared to a theoretical value of 50 cm^{-1}. The separation between the symmetric CH_a and CH_b peaks is 80 cm^{-1} for the experimental data and 60 cm^{-1} for theory. Also note the similarity in the experimental band shapes between the asymmetric CH_b (2825 cm^{-1}) and symmetric CH_b (2601 cm^{-1}) bands. Both have clearly resolved shoulders shifted to the red side by 25–30 cm^{-1} with $\sim 1/3$ the intensity of the main very sharp peak. Comparing the band shapes of the asymmetric CH_a (2762 cm^{-1}) and symmetric CH_a (2521 cm^{-1}) also shows similar envelopes. They also have shoulders, but the red shift is only ~ 7 cm^{-1} and thus not well separated, and their intensities compared to the main peak are larger.

Thus, it seems that on the basis of a comparison of calculated peak separations and experimental separations and on band contours, the assignment of the experimental features between 2500 and 2900 cm^{-1} to the classical structure is reasonable. The most troubling aspect of this assignment is the magnitude of the experimentally observed red shift of the C–H stretches, which is not predicted by theory. The C–H stretches in ethane lie between 2895 and 2985 cm^{-1}. A red shift of close to 400 cm^{-1} is, at first, quite disconcerting. Looking at the situation more carefully, if the classical structure of $C_2H_7^+$ can be represented as a $C_2H_5^+$ loosely attaching a H_2, then the C–H stretches observed would correspond to vibrations in the $C_2H_5^+$ moiety. Much work has been done on the correlation between C–H stretch frequencies, bond lengths, and bond dissociation energies.[48] Caution must be taken when using bond energies to predict vibrational frequencies for cases when the bond dissociation accompanies a significant stabilization energy from the product formed. This

(46) Yardley, J. T. *Introduction to Molecular Energy Transfer*; Academic Press: New York, 1980.
(47) Levine, R. D.; Bernstein, R. B. *Molecular Reaction Dynamics and Chemical Reactivity*; Oxford University Press: New York, 1987.
(48) McKean, D. C. *Chem. Soc. Rev.* **1978**, *7*, 399. See also: McKean, D. C.; Duncan, J. L.; Batt, L. *Spectrochim. Acta* **1973**, *29*, 1037.

leads to a smaller dissociation energy than the frequency alone would seem to indicate. In this particular case, the stabilization energy does not seem to interfere. Instead, the primary complication comes from the interaction of the C–H bonds to give antisymmetric and symmetric stretching modes. The work quantitating a linear relationship between C–H frequencies and dissociation energies uses "isolated" frequencies that are found by deuterating all hydrogens except the one under study. Nonetheless, it is still expected that an estimate for the dissociation energy will serve as a guide for a reasonable first approximation to the stretch frequency. With values from Table I for the difference between the classical and bridged $C_2H_5^+$ forms, a C–H bond energy in the classical structure of $C_2H_5^+$ is calculated to be 82–86 kcal/mol.[49] This is significantly weaker than that in ethane (97.4 kcal/mol) or methane (103.4 kcal/mol). Therefore, a significant red shift in the C–H stretch frequencies in the classical $C_2H_7^+$ structure from those in ethane and methane is expected. From an equation given in ref 48, a C–H bond energy of 84 kcal/mol is predicted to correspond to a stretch frequency of 2770 cm^{-1}. This is between the two observed absorptions that have been assigned to antisymmetric CH_a and CH_b modes. Apparently, the classical structure of $C_2H_7^+$ as calculated by Dupuis has the H_2 moiety more strongly bound to the $C_2H_5^+$ then the structure our experiment suggests, which can be described as $C_2H_5^+ \cdot H_2$.

B. 3400–4200 cm^{-1}. Among the six features above 3400 cm^{-1}, the peaks at 3667, 3726, 3762, 3845, and 3917 cm^{-1} showed no stagnation pressure dependence, whereas the one at 3964 cm^{-1} disappeared at higher pressures. The CO_2 laser was not necessary for any of these features. This lack of CO_2 laser dependence can be explained by realizing that the absorption frequencies (3667–3917 cm^{-1}) correspond to energies (10.5–11.2 kcal/mol) very close to the expected dissociation energy (13 kcal/mol). If the ions initially contain 2–2.5 kcal/mol internal energy or if the dissociation energy measured by Kebarle[25] is too high, then the CO_2 laser photons would not be necessary. On the basis of the vibrational frequencies calculated by Dupuis, an internal energy of 2–2.5 kcal/mol requires an average vibrational temperature of only 400–450 K. Even though the source is cooled with chlorodifluoromethane (Freon-22), a vibrational temperature after the discharge slightly above room temperature is possible.

The fact that the feature at 3964 cm^{-1} disappears simultaneously with the five features below 2900 cm^{-1} strongly suggests that they originate from the same form of $C_2H_7^+$. Therefore, the peak at 3964 cm^{-1} is assigned to a classical $C_2H_7^+$ structure. The five features between 3600 and 3950 cm^{-1} show no pressure dependence, and thus all originate from the more stable bridged $C_2H_7^+$ structure. The fact that these features do not require the CO_2 laser to be present is not an issue here as it was at the lower frequencies as has been discussed above.

Theory does not predict any fundamentals for either the classical or bridged structure above 3600 cm^{-1}.[41] The highest frequency in the classical structure should correspond to the H_1–H_2 stretch vibration of the H_2 moiety which is bound to the $C_2H_5^+$ unit. The unscaled frequency for this motion is 3516 cm^{-1} as compared to 3171 cm^{-1} for CH_5^+ at a comparable level of theory.[41] (At higher levels of theory this mode is predicted to lie at 2797 and 2813 cm^{-1} for CH_5^+.)[41,40] The calculated geometries of the classical $C_2H_7^+$ and CH_5^+ are consistent with the frequency shift. The C–H_1 and C–H_2 bond distances are longer in the $C_2H_7^+$ (1.295 and 1.315 Å)[41] than in CH_5^+ (1.261 Å),[41] and the H_1–H_2 bond distance is shorter in $C_2H_7^+$ (0.824,[41] 0.833 Å[34]) than in CH_5^+ (0.853,[41] 0.882,[34] 0.869 Å[40]). Thus, it's clear that the H–H stretching vibration in $C_2H_7^+$ will be significantly to the blue of that in CH_5^+. Our results indicate that rather than being shifted by only a few hundred wavenumbers, the H–H stretching vibration has actually been shifted close to a thousand wavenumbers to 3964 cm^{-1}. This again suggests a weaker H_2 and $C_2H_5^+$ interaction that causes the H–H stretching frequency to be closer to that of free H_2. In our previous work on the hydrogen cluster ions H_n^+ (n = 5, 7, 9, 11, 13, 15)[50,51] and on the hydrated hydronium cluster ions $H_3O^+ \cdot (H_2O)_n \cdot (H_2)_m$,[52] we were able to detect the H–H stretching vibration in the region from 3900 to 4120 cm^{-1}. The red shift of the H–H stretching vibration from free H_2 (4161 cm^{-1}) was a gauge of the binding energy of the H_2 moiety to the rest of the ion. The most strongly bound cluster ion was H_5^+, which requires ~6 kcal/mol[53] to dissociate into $H_3^+ + H_2$. The red shift of the H_2 stretch was also greatest at 251 cm^{-1}, placing the H_2 stretch at 3910 cm^{-1}. The H_7^+ ion was bound by roughly 3 kcal/mol[53] and showed a red shift of only 181 cm^{-1}, putting it at 3980 cm^{-1}. Since the classical $C_2H_7^+$ is estimated to have a binding energy of ~4 kcal/mol,[25] this places it between H_5^+ and H_7^+. A first approximation to the H_2 moiety frequency, then, is between 3910 and 3980 cm^{-1}. Our peak observed at 3964 cm^{-1} fits neatly into this range.

Table VI. Preliminary Assignments of the Combination Bands for the Bridged Structure of $C_2H_7^+$ (Frequencies Are in cm^{-1})[a]

exptl freq	prelim assgnt	theor freq	species	difference
3917	$2\nu_7$	4148	A	231
3845	$\nu_7 + \nu_{14} + \nu_{17}$	4166	B	321
3762	$\nu_2 + \nu_{17}$	4019	B	257
3726	$\nu_4 + \nu_{17}$	3978	A	252
3667	$\nu_7 + \nu_8$	3860	B	193

[a] Scaled frequencies from ref 41 are used with no anharmonic corrections. Predicted symmetry is C_2.

This feature was also scanned at higher resolution as shown in Figure 7. A P, Q, R band shape emerges. $C_2H_7^+$ is a near-symmetric top with the C–C bond as the top axis. For such a molecule, a transition with a changing dipole moment parallel to the C–C axis would show a P, Q, R band shape. The rotational constant, B, is calculated from the classical $C_2H_7^+$ geometry to be 0.55 cm^{-1}. In fact, the ripples on top of the P and R branches are spaced by 1.1 cm^{-1}, in excellent agreement with the expected $2B$ separation. Using assignments based on these facts, a rotational temperature of 20 K is obtained.

The five features between 3600 and 3950 cm^{-1} are believed to originate from the bridged structure. The six highest calculated frequencies[41] correspond to C–H stretches and can be grouped into three quasi-degenerate pairs. The next highest frequency, ν_7, corresponds to a side-to-side motion of the bridging proton with a scaled frequency of 2074 cm^{-1} and huge intensity of 20 $D^2/(Å^2 \cdot amu)$. The first overtone of this should have an observable intensity and lie close to 4000 cm^{-1}. We tentatively assign the feature at 3917 cm^{-1} to this first overtone. The peak observed at 3667 cm^{-1} has a band contour similar to the feature at 3917 cm^{-1}. The frequency corresponding to the motion of the bridging proton away from the C–C bond is calculated to lie at 1786 cm^{-1}. This leads to preliminary assignment of the 3667-cm^{-1} band as the combination band of the motion of the proton side-to-side and away from the C–C bond ($\nu_7 + \nu_8$). The two smaller features at 3726 and 3762 cm^{-1} are separated by 36 cm^{-1}, close to the separation of the fundamental C–H stretches observed at 3082 and 3128 cm^{-1}. The band contours and relative heights at the three pressures of these two pairs also matches well. This leads to an initial assignment to the combination band of these C–H stretches and ν_{17} which is calculated to have a very strong intensity of 10 $D^2/(Å^2 \cdot amu)$. Even a tentative assignment of the broad feature at 3845 cm^{-1} is difficult. The best guess at this point is a combination band of $\nu_7 + \nu_{14} + \nu_{17}$. The reason for the unusual broadness is unknown. These preliminary assignments are listed in Table VI. Encouraging is the fact that the difference between the experimental frequencies and the theoretical frequencies with no anharmonic correction is between 193 and 257 cm^{-1} for binary combinations and 321 cm^{-1} for the ternary combination. Because the bridged structure calculated for $C_2H_7^+$ has C_2 symmetry, no

(49) Rosenstock, H. M.; Draxl, K.; Steiner, B. W.; Herron, J. T. *J. Phys. Chem. Ref. Data* **1977**, *6*, Suppl. 1, 99, 102.
(50) Okumura, M.; Yeh, L. I.; Lee, Y. T. *J. Chem. Phys.* **1988**, *88*, 79.
(51) Okumura, M.; Yeh, L. I.; Lee, Y. T. *J. Chem. Phys.* **1985**, *83*, 3705.
(52) Okumura, M.; Yeh, L. I.; Myers, J. D.; Lee, Y. T. *J. Chem. Phys.* **1986**, *85*, 2328.
(53) Buehler, R. J.; Ehrenson, S.; Friedman, L. *J. Chem. Phys.* **1983**, *79*, 5982.

combination bands or overtones can be ruled out on the basis of symmetry.

Conclusion

The spectrum of $C_2H_7^+$ has been presented. The spectrum shows a strong dependence both on the ratio of ethane to hydrogen and on the backing pressure used. Evidence has been presented in support of our belief that the different behavior can be attributed to the changing ratio of classical to bridged protonated ethane being probed spectroscopically. The observed infrared frequencies are compared with predicted frequencies for the classical and bridged structures.

Acknowledgment. We thank M. Dupuis for providing us with the results of unpublished calculations. This work was supported by the Director, Office of Energy Research, Office of Basic Energy Sciences, Chemical Sciences Division of the U.S. Department of Energy under Contract No. DE-AC03-76SF00098.

Spectral Evidence of Spontaneous Racemic and "Pseudoracemic" Interactions between Optically Active Poly(pyridyl) Metal Chelates Adsorbed on Smectite Clays

Vishwas Joshi and Pushpito K. Ghosh*

Contribution from the Alchemie Research Centre, Thane Belapur Road, Thane-400601, Maharashtra, India. *Received September 26, 1988*

Abstract: UV-visible absorption and emission spectral studies are reported for enantiomeric (Δ-$(-)_D$, Λ-$(+)_D$) and racemic (Δ,Λ) $Ru(bpy)_3^{2+}$ (bpy = 2,2'-bipyridine) adsorbed on three naturally occurring smectite clays. The results highlight differences in the binding modes of the two forms at low (1-4%) loading levels. The effects of optical purity, loading level, mode of addition of complex, and clay type are also discussed. The observed differences in binding state are ascribed to spontaneous interactions between optical antipodes (racemic interactions). The quenching effect of coadsorbed Δ,Λ-$Co(phen)_3^{2+/3+}$, Λ-$(+)_D$-$Ni(phen)_3^{2+}$, and Λ-$(+)_D$-$Rh(phen)_3^{3+}$ (phen = 1,10-phenanthroline) on the luminescence of Δ-$(-)_D$-, Λ-$(+)_D$-, and Δ,Λ-$Ru(bpy)_3^{2+*}$ is also described. The Stern-Volmer data are rationalized in terms of differences in electron/energy transfer quenching efficiencies between homochiral and heterochiral systems, and luminescence variations arising from binding-state perturbations due to "pseudoracemic" interactions. Such an interpretation is supported by studies with Δ,Λ-$Zn(phen)_3^{2+}$, a structurally analogous, "nonquenching" coadsorbate. Finally, the possible factors that might enhance chiral recognition within clay are discussed.

Optically active poly(pyridyl) chelates of a range of transition-metal ions exhibit a high degree of stereospecificity in binding to DNA[1] and expandable layer lattice (smectite) clays.[2] However, the stereospecificity encountered with the latter is unique in the sense that the clays, being achiral, do not discriminate between enantiomers as such but promote their mutual recognition. This remarkable phenomenon—first reported by Yamagishi[2b]—has led to the development of versatile clay-based systems for optical resolution of racemates[2a,3,4] and for asymmetric synthesis.[5] Recognition between optical antipodes of chelates containing dissimilar metals, e.g., $Ru(phen)_3^{2+}$ and $Co(phen)_3^{2+}$, might also have some bearing on the design of clay-supported bimetallic catalysts from ion-exchanged chiral precursor complexes.[6] The study of clay-chiral molecule interactions is of some fundamental interest as well, since clays might have played an important role in the chiral enrichment process during prebiotic evolution and in the subsequent synthesis of more complex molecular forms.[7,8]

Yamagishi has proposed that poly(pyridyl) metal complexes intercalate in clay as racemic pairs and that this cooperativity for racemic adsorption arises from the rigorous steric requirements essential for closest packing over the clay surface.[2a,c] On the other hand, X-ray powder diffraction studies on Δ,Λ-$Fe(phen)_3^{2+}$-hectorite[9] and time-resolved luminescence studies on Δ,Λ-$Ru(bpy)_3^{2+*}$-hectorite as a function of excitation intensity[10a] have shown that these metal chelates aggregate within the clay matrix even at loading levels as lows as 2% of the cation-exchange capacity. It appeared to us that the twin phenomena of aggregation and racemic pairing may both arise as a consequence of spontaneous interactions between optical antipodes. Preliminary absorption and emission spectral studies on smectite clays lightly loaded with enantiomeric and racemic poly(pyridyl)-Ru(II) chelates have provided strong evidence in support of this hypothesis.[11] In continuation of the above work we report here detailed spectral studies on Δ-$(-)_D$-, Λ-$(+)_D$-, and Δ,Λ-$Ru(bpy)_3^{2+}$ adsorbed on three naturally occurring smectite clays and contrast these findings with those of the complex adsorbed on micellar

(1) (a) Barton, J. K. *Science* **1986**, *233*, 727, and references therein. (b) Yamagishi, A. *J. Phys. Chem.* **1981**, *88*, 5709.

(2) (a) Yamagishi, A. *J. Coord. Chem.* **1987**, *6*, 131. (b) Yamagishi, A.; Soma, M. *J. Am. Chem. Soc.* **1981**, *103*, 4640. (c) Yamagishi, A. *J. Phys. Chem.* **1982**, *86*, 2472. (d) Yamagishi, A.; Fujita, N. *J. Colloid. Interface Sci.* **1984**, *100*, 1778. (e) Turro, N. J.; Kumar, C. V.; Grauer, Z.; Barton, J. K. *Langmuir* **1987**, *3*, 1056, and references therein.

(3) Yamagishi, A. *J. Am. Chem. Soc.* **1985**, *107*, 732.

(4) Kotkar, D.; Ghosh, P. K. *Inorg. Chem.* **1987**, *26*, 208.

(5) (a) Yamagishi, A. *J. Chem. Soc., Chem. Commun.* **1986**, 290. (b) Yamagishi, A.; Aramata, A. *J. Chem. Soc., Chem. Commun.* **1984**, 452.

(6) Efficient hydrogenation catalysts can be obtained from clays exchanged with poly(pyridyl) Ru and Rh chelates, through calcination and subsequent activation under hydrogen (Kotkar, D.; Joshi, V.; Ghosh, P. K., unpublished results).

(7) (a) Tsvetkov, F.; Mingelgrin, V. *Clays Clay Miner.* **1987**, *35*, 391, and references therein.

(8) (a) Cairns-Smith, A. G. *Sci. Am.* **1985**, *252*, 74. (b) Bernal, J. D. *The Origin of Life*; Weidenfeld & Nicholson: London, 1967; p 57. (c) Ponnamperuma, C.; Shimoyamaad, A.; Friebele, E. *Origins Life* **1982**, *12*, 9. (d) Weiss, A. *Angew. Chem., Int. Ed. Engl.* **1981**, *20*, 850.

(9) Berkheiser, V. E.; Mortland, M. M. *Clays Clay Miner.* **1977**, *25*, 105.

(10) (a) Ghosh, P. K.; Bard, A. J. *J. Phys. Chem.* **1984**, *88*, 5519. (b) Similar aggregation effects have also been reported for an anionic Ru(II) chelate intercalated in synthetic hydrotalcite clays. (Giannelis, E. P.; Nocera, D. G.; Pinnavaia, T. J. *Inorg. Chem.* **1987**, *26*, 203). (c) Aggregation effects are not unique to poly(pyridyl) metal chelates. Aggregation of organometallic complex "pillars" on synthetic fluorhectorite and montmorillonite has also been reported (Tsvetkov, F.; White, J. *J. Am. Chem. Soc.* **1988**, *110*, 3183).

(11) (a) Joshi, V.; Kotkar, D.; Ghosh, P. K. *J. Am. Chem. Soc.* **1986**, *108*, 4650. (b) Joshi, V.; Ghosh, P. K. *J. Chem. Soc., Chem. Commun.* **1987**, 789.

0002-7863/89/1511-5604$01.50/0